FULL RESEARCH ARTICLE

Comprehensive characterization of mechanical and physical properties of PLA structures printed by FFF-3D-printing process in different directions

Giulia Morettini[1] · Massimiliano Palmieri[1] · Lorenzo Capponi[1] · Luca Landi[1]

Abstract

The industrial interest in additive manufacturing (AM) techniques is currently increasing for the realization of functional mechanical components. For this reason, the structural simulation of parts or complete structures made using this new manufacturing technique is gaining considerable importance. To realise accurate finite element models for the purpose of predicting the dynamic or static behaviour of the component printed and avoid unexpected failures, it is necessary to be aware of some mechanical and physical properties of the print material. Unfortunately, in the literature, it is very difficult to find all the data necessary to perform static or dynamic simulations of 3D printed parts. In this context, this activity aims to determine all these mechanical and physical properties for parts made in White-Pearl Polylactic-acid (PLA) Ultimaker filament using the Fused Filament Fabrication (FFF) technique. A set of printing parameters was chosen and kept constant in all tests which, based on literature data, maximizes the static strength and the fatigue limit of the component. Only the building direction was varied to increase the applicability of the obtained results to any geometry. The main results found for the horizontally moulded specimens (representing the best constructive solution) are the Ultimate Tensile Strength equal to 57.15 MPa, the elastic modulus 2606 MPa, the fatigue limit evaluated at 2×10^6 cycles equal to 13.5 MPa, the damping and density of the material of 0.008 dimensionless value and 1.1246 g/cm^3, respectively. Only thanks to the obtained results, finite element models can be developed for reliable static and dynamic analysis.

Keywords Additive manufacturing · Polylactide PLA · Mechanical behaviour · Tensile test · Fatigue test · DMA test

1 Introduction

Nowadays, thanks to its wide applicability, plastics are used in almost all industrial sectors [1]. In some cases, owing to its many well-known advantages, plastics have even replaced components usually produced by ferrous material [2]. Additive manufacturing (AM) easily fits into this scene. Indeed, thanks to its ability to transform designers' ideas into successful prototypes, without any geometric limitations, the interest in additive manufacturing technology has rapidly grown [3–8]. In this context, the current challenge is to bring AM closer to conventional manufacturing processes, by supporting the industrial production line in ordinary manufacturing or, with a future vision, by replacing it completely [9]. However, why is this not happening yet?

Since the 1990s, companies have focused their attention on trying to increase the level of productivity while reducing manufacturing costs [10]. Certainly, the fused filament fabrication (FFF), which is arguably one of the most widely used 3D-printing technologies [11, 12], does not fully reflect these manufacturing needs.

However, while manufacturing needs can be compensated by the flexibility of the process [13, 14], 3D fabricated components still do not find a clear definition in their mechanical or physical properties due to the many settable variables that affect the printing process [15, 16] and this aspect also concerns the metallic materials [17].

The latter problem is certainly the main cause that does not allow this new technology to make the production leap. In fact, to estimate the static and dynamic behavior of components by finite elements numerical models [18] a concise and explicit definition of the mechanical and physical

✉ Giulia Morettini
giulia.morettini@unipg.it

1   Department of Engineering, University of Perugia, Via G. Duranti 93, 06125 Perugia, Italy

properties of a component 3D manufactured is of fundamental importance.

To address this need, in recent years, several researchers have extensively investigated and discussed the influence of the most important FFF-printing parameters [19] or production procedures [20], mainly taking as a reference the maximization of the ultimate tensile strength or the fatigue limit, trying to define an optimal printing parameter set [21–24].

Unfortunately, however, it is very difficult to find, for a single set of printing parameters, all the information regarding the physical and mechanical properties of a specific material. For these reasons, this research activity aims to experimentally determine the most important mechanical and physical properties of the White-Pearl PLA manufactured through a commercial 3D printer Ultimaker 3 Extended trying to make up for this lack. In addition, three printing directions will be taken into consideration to leaving the reader with the best choice of orientation, on the printing plate, of the part to be produced.

To be more specific, the main data collected in this study are the density of the material printed, the Ultimate Tensile Strength (UTS), the elastic moduli (derived from the tensile or bending test), the damping, the Wöhler curve of the material used and consequently the fatigue limit evaluated at 2×10^6 cycles.

All the experimental tests were conducted following the appropriate ASTM or ISO standard regulations. The obtained results are thus useful for designers and engineers to make reliable static or dynamic model of 3D printed PLA mechanical components in White-Pearl PLA.

The printing parameters reported in Table 1 are kept constant. The choice of these is fundamental and was deduced from an accurate and detailed literature analysis described in the following chapter; in this way, the reader can easily use them to manufacture any component. Chosen printing

parameters and settings are those that, according to various authors [10, 16, 23–27], maximize the UTS, the fatigue limit, or the elastic modulus.

Ultimately, thanks to this research activity designers and engineers can realize robust and reliable static or dynamic models of 3D printed PLA mechanical components in White-Pearl PLA.

2 Materials and methods

2.1 Material and printing parameters

The specimens tested were additively manufactured through the commercial printer Ultimaker 3 Extended, using FFF Technology. In this study, different specimens were fabricated by melting, through a nozzle of 0.4 mm diameter, a PLA filament of 2.85 mm diameter commercially available of pearly white colour (cod.1625) produced by Ultimaker. The interface between CAD geometry and G-Code of the printer is guaranteed by the open-source slicing application *Cura 4.7.*

The choice of the process parameters is of extreme importance for the success of printing, especially if the aim is to obtain components that possess load capacity. In the literature, there are many studies on the influence of these parameters on the mechanical or physical characteristics of printed material. Tymrak et al. [26] show how the use of a layer of 0.2 mm thickness, with an Infill Line Directions of (0, 90) degrees maximizes the UTS of the PLA. With their work, [27] Cristian and Dudescu confirm that this setting provides the greatest ultimate tensile strength. Abeykoon [16] instead investigates how the temperature variation of the nozzle, the Infill speed, Infill pattern, and the Infill density affect the tensile performance. His research activity identifies, in the set [215 °C; 90 mm/s; linear; 100%], the best UTS for printed PLA. According to Ezeh and Susmel [10], the infill density of 100% also maximizes the fatigue limit of PLA. Moreover, it is commonly recognized that setting the Infill layer thickness equal to the height of the layer, reduces the presence of voids and discontinuities in the material.

Unfortunately, however, no article is available in the literature that unambiguously defines a set of print parameters that at the same time maximizes all the most important mechanical and physical properties. In fact, as already mentioned, this could be useful to address a numerical finite element analysis of FFF printed components with this material. The authors have, therefore, created a particular parametric set (starting from the set of "Fine Default" process parameters available in the Cura software) exploiting all the parametric optimization results listed in the previous lines to obtain the best setting solution for printing. Table 1

Table 1 Set of used process parameters

Quality	Layer height	0.2 mm
Shell	Wall line Count	2
	Top/bottom thickness	1 mm
	Top/bottom layers	2
Infill	Infill density	100%
	Infill pattern	Lines
	Infill line directions	[0, 90]
	Infill layer thickness	0.2 mm
Material	Printing temperature	215 °C
	Build plate temperature	60 °C
Speed	Print speed	90 mm/s
	Cooling fan speed	100%

summarises the parameters used and kept always constant during the production of the different specimens.

2.2 Specimens

This section will present in detail the geometric values for the realization of the different specimens suitable for each mechanical characterization test. Whenever possible, these will refer to the reference ASTM standards. The aim is to provide the reader with as much information as possible to replicate the test and the designer with a universally recognized result.

2.2.1 Dog-bone specimens for tensile and fatigue test

The manufacturing of these dog-bone flat specimens was done in accordance with the ASTM D638-14 reference standards for the tensile test [28] and D7791-17 for the fatigue test [29]. In both test cases, tensile or fatigue, the type I specimen was chosen, the geometric data of which are shown in Fig. 1. Due to the material anisotropy, for the tensile test, 6 specimens for three print directions (horizontal, side, vertical) were printed, as shown in Fig. 2, for a total of 18 specimens. For the fatigue test, instead, 2 test specimens were printed in the horizontal direction, for each of the three stress levels tested, a specimen always manufactured in the horizontal direction, was instead dedicated to the search for the fatigue limit. Therefore, a total of 7 specimens were produced to perform the fatigue test.

For all samples, after contour removal, the corners and the surfaces were smoothed using fine sandpaper (in accordance with ASTM D638-14 6.4). After this procedure, all the surfaces of the specimens found to be free of visible defects, scratches, or imperfections. After the cleaning process, the surface of all the specimens was marked by the gripping line which identifies the correct location of where the clamps ought to be placed (gray area of Fig. 1). Only the 18 tensile specimens were also marked with the extensometer line, which similarly identifies the correct point to place the extensometer (dashed lines in Fig. 1).

2.2.2 Specimen for dynamic mechanical analysis (DMA) tests

The DMA specimens were produced in accordance with the geometric definition of ASTM D5023-15 [30], in which the various parts specify methods for determining the dynamic mechanical properties of rigid plastics within the region of linear viscoelastic behavior. Three test specimens were manufactured in each direction (vertical, horizontal and on-side) to be used for three-point bending measurements at a single temperature but varying the excitation frequency from 0 to 100 Hz. The geometrical dimensions of the specimen are shown in Fig. 3.
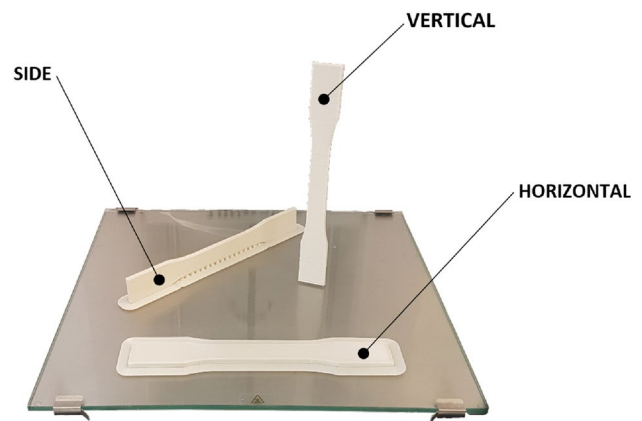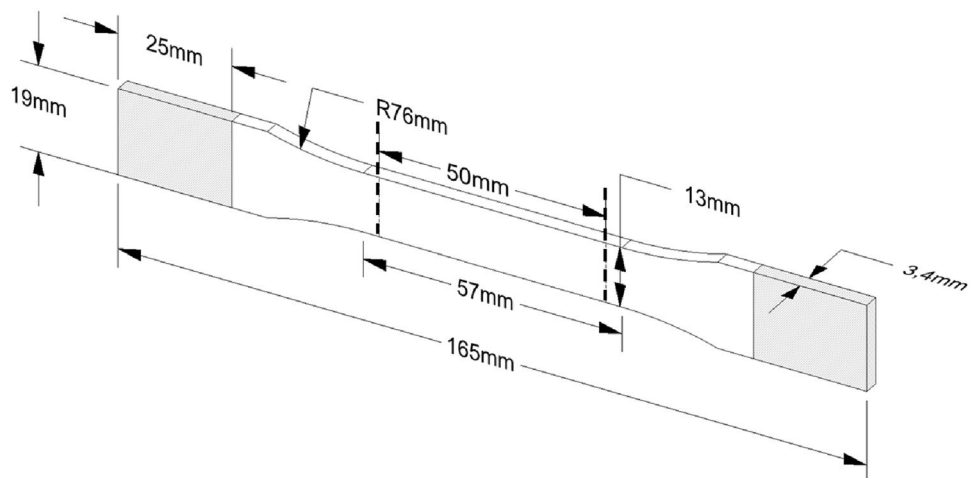

Fig. 2 Real specimens (for fatigue or tensile test) on the print plate

Fig. 1 Specimen type I dimensions in accordance with ASTM D638-14 and D7791-17 standards for tensile and fatigue test
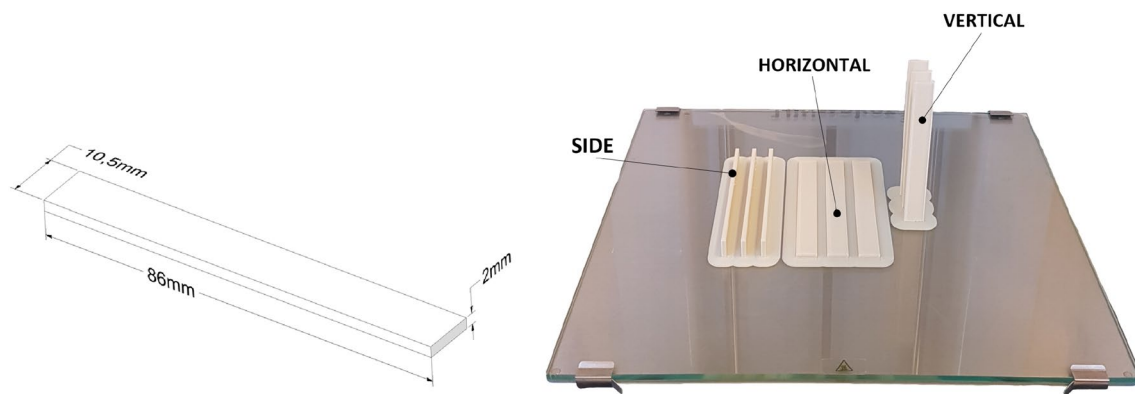
Fig. 3 DMA specimen dimensions in accordance with ASTM D5023-15 standards for three-point bending DMA, test and real specimen on the print plate
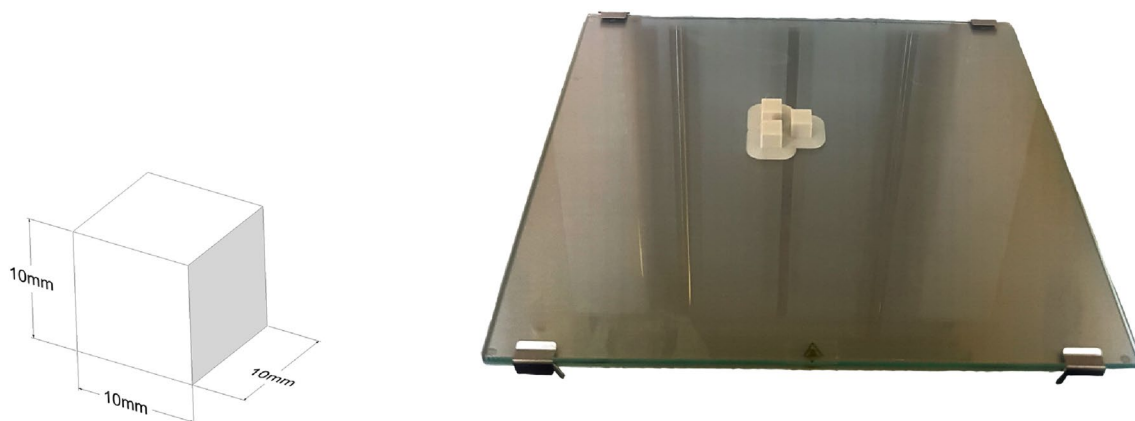

Fig. 4 Specimen dimension for the density evaluation and real specimen on the print plate

2.2.3 Specimens for the determination of density and damping

Finally, the specimens were made to carry out the tests to evaluate the real density of the material. The geometric dimensions of the specimens are shown in Fig. 4. To carry out the tests, three specimens were printed. Since the dimensions of these specimens are cubic, the printing direction does not affect the test.

2.3 Experimental setting and procedure

2.3.1 Density evaluation

Density, was derived from mass and real volume of the solid, is a property that is conventionally measured to identify a physical property, to track physical changes in a sample, to indicate the degree of uniformity among different sampling units or specimens, or to indicate the average of a large item.

This property has a dominant influence on the dynamic behavior of a system. In additive manufacturing techniques, density changes are due to many factors: the localized differences in crystallinity, loss of material, thermal history, porosity, different composition of the original filament, or other causes related to a specific set of printed parameters [31]. In this work, a simple determination of the mass in the air of a standard specimen printed was done using an Ohaus Pioneer weight scale with high accuracy (readability of 0.0001 g) and repeatability performance for applications in the laboratory.

2.3.2 Tensile test

The tensile test, also known as the tension test, [27] is a fundamental quasi-static test of materials science and engineering in which a sample is subjected to a controlled increasing tension until failure. The primary mechanical properties of the material tested are derived from the results of that test. This test was conducted to get to know the UTS,

elastic modulus (also known as Young's modulus), maximum strain, and maximum elongation percentage for the three build directions analysed.

The printed specimens were tested under quasi-static tensile loading at room temperature and humidity of 50%, using a load controller Instron 3382 testing machine with a 100 kN load cell. All the specimens, for each print direction, were tested at a chosen constant displacement rate of 2 mm/min (as indicated by the corresponding standard ASTM D638 [28]) and, during the test, the local strain was measured using a standard Instron W-6280 axial extensometer having gauge length equal to 50 mm.

2.3.3 Fatigue tests

The aim of this section is to investigate and record the Wöhler curve and the fatigue limit of the material of PLA specimens printed in horizontal positions. Since there are no specific standards focusing on fatigue testing of plastic AM materials [10], the ASTM D7774 standard [32], that regulates the test method for uniaxial fatigue proprieties for Plastics was used as a reference.

All the fatigue specimens were tested in an Instron MODEL 1342 testing machine, performing a stress control tension–tension fatigue test at constant maximum loading with a stress ratio $R = 0$. To draw the Wöhler curve of the

evaluation of the complex bending modulus E_b^* performing a 3-point bending test. This parameter can be defined as

$$E_b^* = E' + iE'' \tag{1}$$

where E' and E'' are the storage (also called elastic) modulus and the loss modulus, respectively. The storage modulus E' describes the elastic property of the material, while the loss modulus E'' the viscoelastic properties.

While the elastic bending modulus E_b, which is calculated from the slope of the initial part of a bending stress–strain curve, is conceptually similar to the storage modulus E', they are not the same. However, if the DMA tests are done in the same direction as the bending test, in the absence of other significant test results, the results of storage modulus should be very close to the elastic bending modulus E_b:

$$E_b \cong E'. \tag{2}$$

Then, the loss factor ι, which defines the hysteresis of the viscoelastic processes, can be derived as

$$\iota = \tan(\delta) = \frac{E''}{E'} \tag{3}$$

where δ is the phase shift angle between the stress and strain. Finally, the relationship [33] between the complex bending modulus E_b^*, the stress amplitude σ_0, the strain amplitude ϵ_0 and the phase shift δ is given by Eq. (4):

$$E_b^* = \frac{\sigma}{\epsilon} = \frac{\sigma_0 \sin(\omega t + \delta)}{\epsilon_0 \sin(\omega t)} = \frac{\sigma_0 \sin(\omega t)\cos(\delta) + \sigma_0 \cos(\omega t)\sin(\delta)}{\epsilon_0 \sin(\omega t)} = \frac{\sigma_0}{\epsilon_0}(\cos(\delta) + i\sin(\delta)) \tag{4}$$

material a frequency of 4 Hz (in accordance with the relative standard) has set and a standard routine test is chosen with an endurance limit of 2×10^6 cycles.

Four load levels were investigated $\sigma_{\max} = \begin{bmatrix} 24\text{MPa}, & 20\text{Mpa}, & 16\text{MPa}, & 13\text{ MPa} \end{bmatrix}$ and the relative number of failure cycles recorded. The data to be obtained from this test are principally the fatigue limits $\sigma_{\max}^{\lim}$, at 50%, 10% and 90% of survival probability calculated at 2×10^6 number of cycles, the negative inverse slope K, and the intercept C (parameters, the latter, essential for the expression of the Wöhler curve as $C = N\sigma^K$).

2.3.4 Dynamic mechanical analysis

The Dynamic mechanical analysis (DMA) is a measurement technique that allows the experimental assessment of some mechanical properties of the material tested [33, 34] as the excitation frequency varies. In particular, this test allows the

The experimental campaign was designed to obtain the values of the elastic bending modulus E_b and the loss factor ι, but above all the damping ζ of the PLA samples in the 3 build directions with a 3-points bending test. This latter result is the most important for the ultimate purpose of our manuscript. In fact, only thanks to the knowledge of the material damping it is possible to numerically simulate the dynamic response of a real molded component.

As suggested by BS ISO 4664 [35] standard, it is possible to correlate the loss factor ι with, the ratio of decay of amplitude in the free vibration analysis Λ, defined as logarithmic decrement, which is a measure of energy dissipation in the time domain analysis [36]:

$$\Lambda = \frac{\left(1 - \sqrt{1 - \iota^2}\right)2\pi}{\iota} \tag{5}$$

The logarithmic decrement Λ is dimensionless and is another form of the dimensionless damping ζ. Once Λ is known, ζ can be found by solving the Eq. (6) [37]:

$$\zeta = \frac{\Lambda}{\sqrt{(2\pi)^2 + \Lambda^2}} \tag{6}$$

Each particular DMA test was performed with a Mettler Toledo machine and repeated on 3 different samples under the same conditions, for a total of 9 specimens tested. The experiments were conducted with a constant applied force of 1 N in 0–100 Hz frequency range (5 Hz of step) at room temperature. The maximum amplitude displacement was limited at 500 um.

3 Results and performance evaluation

3.1 Density evaluation

The density was calculated using the weight of the specimen and the real printed volume. Table 2 shows the measurements for the three specimens used.

The mean value recorded was 1.1246 g/cm³, if this value is compared with the one reported by the technical PLA White-Pearl datasheet filament, equal to 1.238 g/cm³, is evident that the density of the specimens produced decrease by 9.1% with respect to that of the pure PLA filament. It is in fact, recognized in the literature [31], that a specific set of print parameters influence the density of the specimen printed.

Carrying out the evaluation of the real density of the samples (often neglected) is a simple but very important test. In fact, density is a fundamental parameter for the designer who wants to statically or dynamically simulate the behavior of a component or of an entire structure. If you want to carry out a correct numerical simulation, this parameter must be known in advance by correlating it to a specific set of printing parameters.

3.2 Tensile test

The authors used the ASTM D638 [28] as the reference standard for the determination of the mechanical properties that were measured via a tensile test. The stress–strain diagrams resulted from the three build directions are shown in Fig. 5. These diagrams make it clear that, as can be expected, the build direction affects the strength of 3D printed parts.

The results obtained and the other mechanical properties obtained from the post-processing of the data, are summarized in Table 3 in terms of maximum strain, breaking load, elastic modulus (or rather Young's modulus), and percentage of maximum elongation.

Specifically, for each mechanical property, the mean values and the standard deviations are reported to better analyse the mechanical behaviour of the different manufacturing conditions and the dispersion of the data.

From the first analysis, we can state that all of the experimental results are comparable with data present in literature. In particular, the Horizontal specimens have the highest UTS stress level equal to 57.15 MPa, this result is very similar to the UTS equal to 58 MPa of PLA produced by conventional methods [41] and is in line with the results reported in the literature by Bledzki [38] or Wittbord [39]. Even the ultimate tensile strength of the printed specimen on the Side does not differ much from the result obtained from the Horizontal specimen, while the vertical specimens are those that most deviate from it: their UTS is 58.24% lower. This deviation is also confirmed by the studies of Laureto [40] which, tank to his study, affirm that: vertical tensile specimens had an ultimate tensile strength 47.9% less than horizontal. This particular behavior, known in literature, is mainly due to the evidence that the variation of the build direction alters the extruded filament alignment with loading, and this significantly affect tensile strength [26].

This behaviour can be further highlighted if we compare the maximum strain and the and maximum elongation percentage for the three different sets: as we can see from Fig. 5c the vertical specimens present a brittle behaviour. Using an optical analysis of the fracture surface of the vertical specimen, it is evident that the detachment occurred by separating two consecutive layers. The horizontal specimens and those arranged on one side, on the other hand, as visible in Fig. 5a, b exhibit a ductile behaviour and their fracture surface is comparable to that of a homogeneous material.

From these considerations it is clear that the material behaves in an anisotropic way. Therefore, during the design of real components, the reciprocal relationship between the load and the orientation of the layers must be considered, differing the limits of the static loads associated with the stress direction.

Albeit, in all the analysed cases the Young's moduli values remain within the standard range declared by the PLA supplier. This means that, if during the design phase we remain in the linear elastic loading field, we will make a negligible error if we consider the PLA analysed as a homogeneous isotropic material.

In support of these results we can report, for completeness, the value of the Poisson's coefficient $\nu = 0.36$ taken from reference [42].
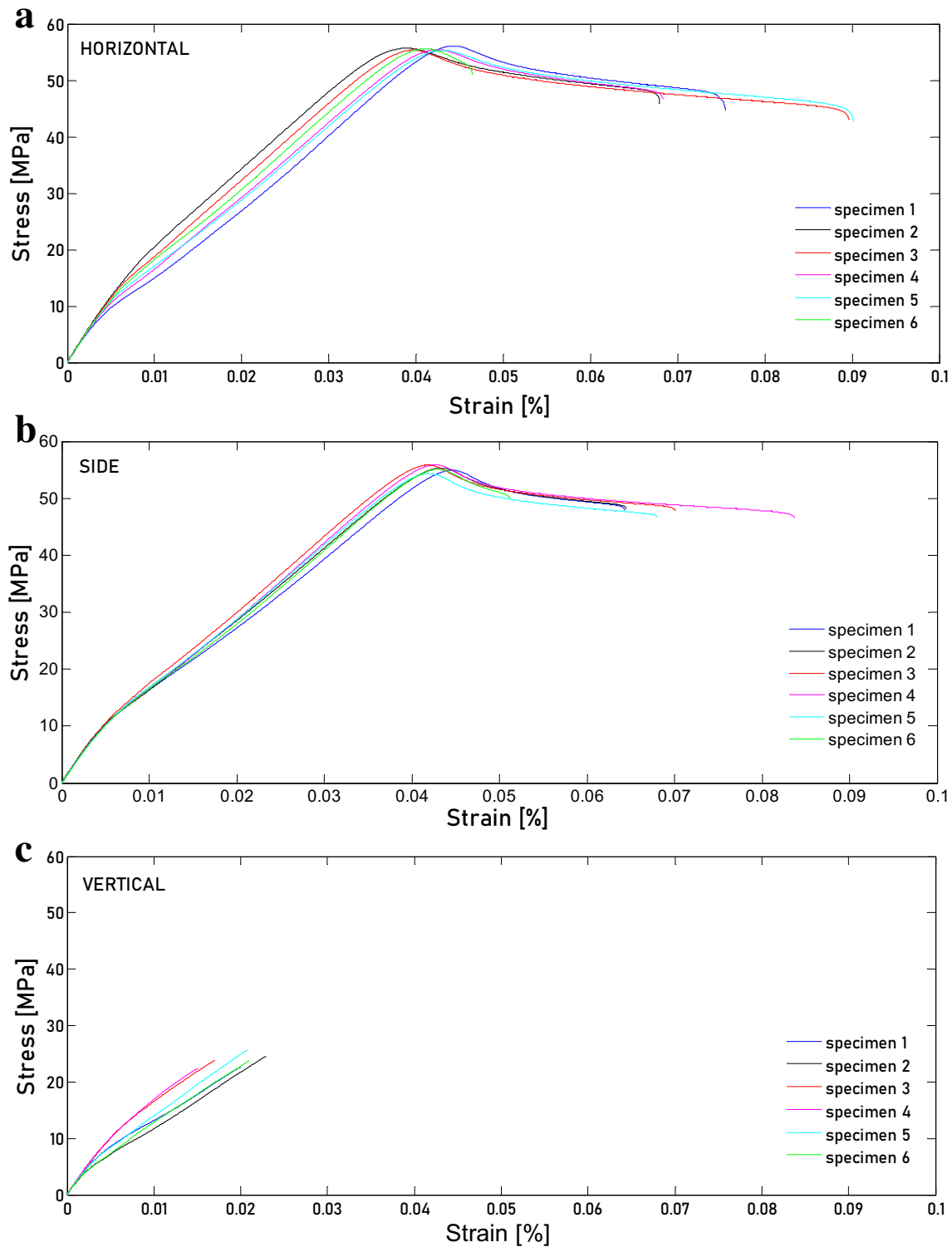
Table 2 Results of density measurement of the mass in air of a standard specimen printed

	Specimen 1	Specimen 2	Specimen 3	Mean value
Real volume [cm³]	1.0915	1.0907	1.0911	1.0911
Weight [g]	1.2363	1.2171	1.2280	1.2271
Density [g/cm³]	1.1326	1.1158	1.1254	**1.1246**

Fig. 5 Stress–strain curves results for the three build directions for the 18 tensile test specimens

3.3 Fatigue test

The S–N approach is widely accepted in the engineering community, as a reference for the design of thermoplastic components when considering the dynamic excitation of a component [15]. For this reason the results of the fatigue test are summarized in the S–N charts of Fig. 6, where a statistical elaboration of the data is presented in terms of

Table 3 Mean values and standard deviation of the principal post elaboration results of tensile test

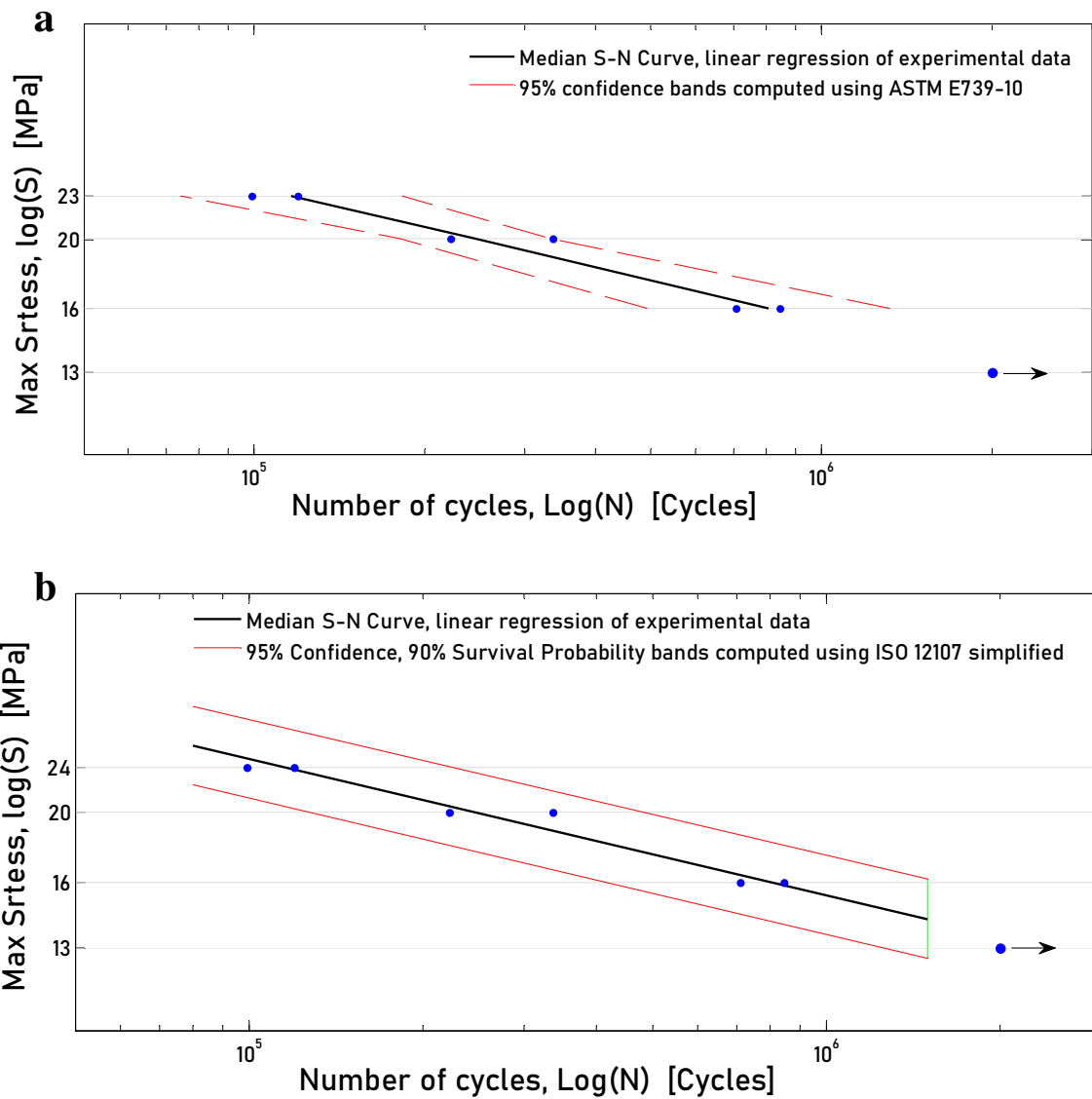|	Maximum strain [mm/mm]		Ultimate tensile strength [MPa]		Young's modulus [MPa]		maximum elongation percentage [%]	
	Mean value	Standard deviation	Mean value	Standard deviation	Mean value	Standard deviation	Mean value	Standard deviation
Horizontal (H)	0.0428	0.002	57.15	0.19	2606	94	4.36	0.21
Side (S)	0.0389	0.002	55.83	0.53	2438	74	4.13	0.09
Vertical (V)	0.0167	0.005	24.22	1.11	2380	72	1.02	0.18

Fig. 6 Results of the fatigue tests. **a** 95% confidence bands computed using ASTM E739-10. **b** 95% confidence, 90% survival probability bands computed using ISO 12107 simplified

maximum stress against the number of cycles corresponding to failure. An arrow marks the "run out" specimen, or better, the specimen that has not broken but has exceeded the minimum cycles limit that marks the beginning of indefinite life.

The test results were elaborated in two graphs following the reference standards. In Fig. 6a, the linear regression results (black line) are reported with the confidence bands of 95% (red lines) computed using ASTM E739 indication [43]. Instead, following, the ISO 121107 standard, in Fig. 6b, the same regression line is reported with the bands (red lines) that take into account the combination of the probability of survival equal to 10–90% and the confidence equal to 95%. All the tested specimens fall within the confidence and/or probability bands used, a symptom of the fact that there is no great variability in the results. This is also confirmed by the low value of the standard deviation on the number of recorded cycles.

From the data, it is possible to extrapolate the fatigue limits $\sigma_{MAX50\%}^{\lim}$, $\sigma_{MAX10\%}^{\lim}$ and $\sigma_{MAX90\%}^{\lim}$ corresponding to 50% 10% and 90% of survival probability calculated at 2×10^6 number of cycles, the negative inverse slope K and the intercepts C parameters for the expression of the Wöhler curve as $C = N\sigma^K$ and the scatter index t_σ. All the results are summarised in Table 4.

The fatigue limit and the negative inverse slope of printed PLA fall within the conventional range of fatigue limits for PLA produced in a conventional manner [41]. It is, therefore, possible to state that AM is suitable for engineering PLA components showing a fatigue performance comparable to the one characterizing structures fabricated using conventional technologies. However, during the design phase, the engineer must take into account to arranging the component in the printing plate so that the fatigue-prone parts are printed horizontally. This is because it is unequivocally recognized that horizontal printing produces (under the same conditions) higher fatigue limits [44–46].

From a macroscopic viewpoint, the process of fatigue failure in thermo-polymers, resembles that of metals [47, 48]. The fracture site, in the greater length of the specimens, varies randomly.

3.4 Dynamic mechanical analysis

The resulting values of the DMA test are shown in Fig. 7 for each of the three directions (i.e., horizontal, side, and vertical), the data obtained from the three specimens tested (represented by dots) were averaged and plotted with a continuous line over the considered frequency range [35, 36].

In particular, if we refer to Fig. 7a, we can appreciate that for all the specimens tested, in each direction, the Elastic bending Modulus values are constant over the excitation frequency analyzed. The loss factor is shown in Fig. 7b (and, thus, the damping ratio); instead, presents an unstable behavior in the frequency range investigated.

As shown in Fig. 7a, the difference between the bending elastic modulus of specimens printed on Side and Vertically is about 22%; this means that, also in the analysis case, the vertical direction turns out to be the most unfavorable for the mechanical properties of the system. This result confirms the fact that inter-layer cohesion represents the point of the major critical issue of the system. The bending excitation of the vertical specimens, on the testing machine, in fact, causes a state of stress normal with respect to the individual print layers of vertical specimens unlike specimens printed on one side or horizontally, where, during the test, the extruded filaments are stressed.

Figure 7b instead highlights a less marked gap between the three cases under examination, especially at low frequencies. This is due to the fact that the loss factor is a global feature of the system that could be less influenced by the stratification of the specimen. The graphic trend shows maximum values around 85 Hz; therefore, at this frequency, the material (and the microstructure built by the additive process) has the best performance in terms of mechanical energy absorption.

The results of the DMA test are summarised in Table 5; from this, it is possible to affirm that: the specimens' tests confirm that the additive manufacturing process, generates anisotropic behavior of the structural elements fabricated.

The results obtained from this test are extremely important for the optimization of the structural element performances produced using the additive manufacturing

Table 4 Mechanical characteristics result of fatigue test. Horizontal specimens

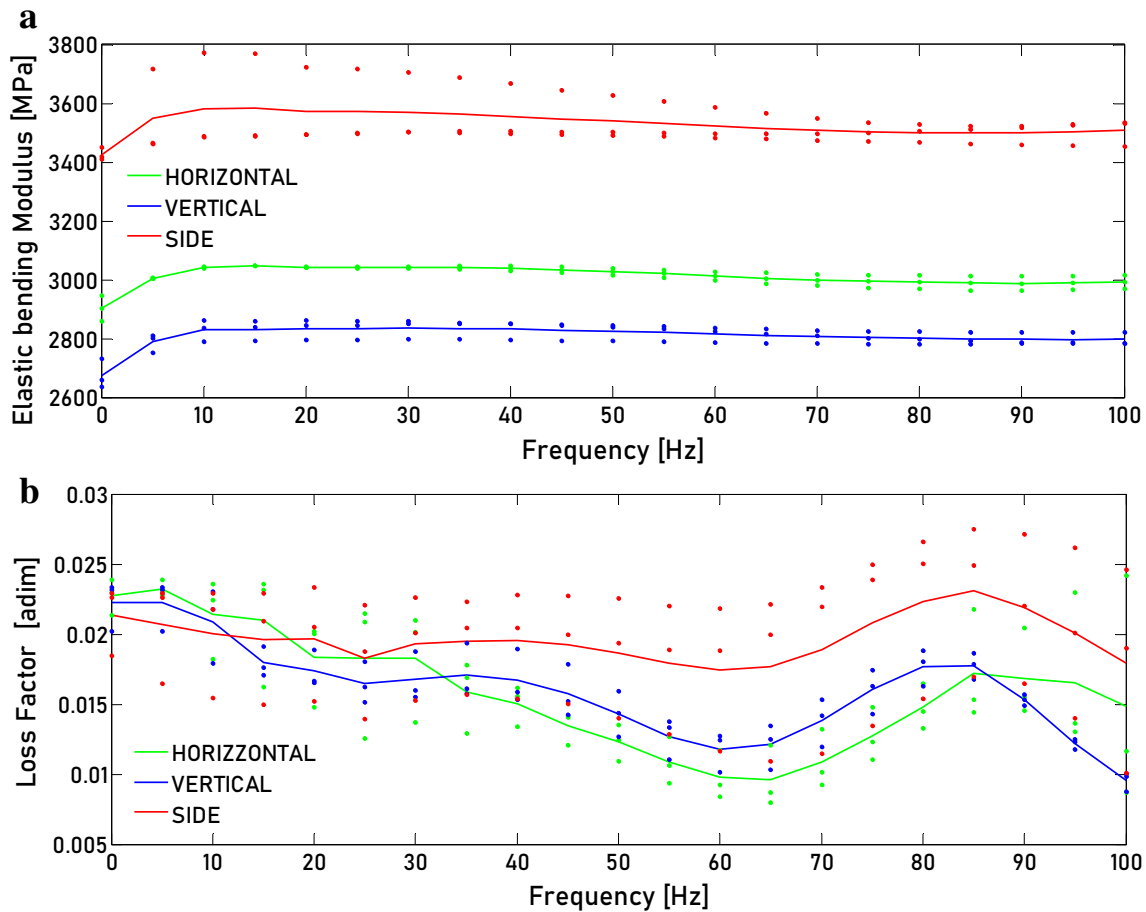| Negative inverse slope	Intercepts	Standard deviation of Number of cycles	Fatigue limit at 10% of probability	Fatigue limit at 50% of probability	Fatigue limit at 90% of probability	Scatter index
K	C	σ_{Nc}	$\sigma_{10\%}^{\lim}$	$\sigma_{50\%}^{\lim}$	$\sigma_{90\%}^{\lim}$	t_σ
		[cycles]	[Mpa]	[Mpa]	[Mpa]	–
5.3358	2.1461 10^{12}	0.103	11.9	13.5	15.3	1.3

Fig. 7 3-points bending results of DMA test

Table 5 Mean mechanical characteristics resulting from DMA test

	Elastic bending modulus	Loss factor	Damping
	E_b	ι	ζ
	[MPa]	[adim]	[adim]
Horizontal (H)	2805	0.0158	0.008
Side (S)	3563	0.0218	0.011
Vertical (V)	3012	0.0157	0.008

technique. In Particular, for a designer, the knowledge of material damping is the only way to predict the behavior of a mechanical component must survive to a dynamic (cyclic or random) loading in the machines, where it is used. In fact, to perform a reliable numerical dynamic analysis of a system every finite elements software needs knowledge of materials damping value to optimize the new design.

4 Conclusions

In the present paper, a concise and explicit definition of the mechanical and physical properties of PLA material printed using a White-Pearl Ultimaker filament and an Ultimaker 3 Extended printer with a well-defined set of printing parameters was done. Principally three printing directions of growth were investigated, to arrive to a competitive definition of both physical and mechanical properties of this material. In particular, this experimental research activity is thought to compensate for the lack of literature data concerning the dynamic behavior of the PLA material, by evaluating not only the fatigue limit but also the damping coefficient of the material used. Only thanks to the results summarised in the present paper, all the data necessary to future perform static or dynamic simulations of 3D printed parts are now available to the designer who wants to create finite element models of components made by an Ultimaker 3 Extended printer with a White-Pearl PLA Ultimaker filament. Now new research possibilities are to be opened: investigating for example the random vibrational fatigue behavior of molded

components, a topic that could not be addressed without the results of this research.

Availability of data and material Not applicable.

Code availability Not applicable.

Declarations

Conflict of interest On behalf of all authors, the corresponding author states that there is no conflict of interest concerns this research.

References

1. Juarez JL (2003) A methodology for transitioning from metallic parts to plastic injected components. ETD Collection for University of Texas, El Paso. AAIEP10567. https://scholarworks.utep.edu/dissertations/AAIEP10567

2. Landi L, Stecconi A, Morettini G, Cianetti F (2021) Analytical procedure for the optimization of plastic gear tooth root. Mech Mach Theory. https://doi.org/10.1016/j.mechmachtheory.2021.104496

3. Allevi G, Capponi L, Castellini P, Chiariotti P, Docchio F, Freni F, Tomasini EP (2019) Investigating additive manufactured lattice structures: a multi-instrument approach. IEEE Trans Instrum Meas 69(5):2459–2467

4. Montanini R, Rossi G, Quattrocchi A, Alizzio D, Capponi L, Marsili R, Tocci T (2020) Structural characterization of complex lattice parts by means of optical non-contact measurements. In: 2020 IEEE International Instrumentation and Measurement Technology Conference (I2MTC). IEEE, pp 1–6

5. Luo Y, Chen Y (2021) FPGA-based acceleration on additive manufacturing defects inspection. Sensors 21(6):2123

6. Allevi G, Castellini P, Chiariotti P, Docchio F, Marsili R, Montanini R, Tomasini EP (2019) Qualification of additive manufactured trabecular structures using a multi-instrumental approach. In: 2019 IEEE International Instrumentation and Measurement Technology Conference (I2MTC). IEEE, pp 1–6

7. Arh M, Slavič J, Boltežar M (2021) Design principles for a single-process 3d-printed accelerometer–theory and experiment. Mech Syst Signal Process 152:107475

8. Barši PT, Slavič J, Boltežar M (2020) Process parameters for FFF 3D-printed conductors for applications in sensors. Sensors 20(16):4542

9. Bikas H, Stavridis J, Stavropoulos P, Chryssolouris G (2016) A design framework to replace conventional manufacturing processes with additive manufacturing for structural components: a formula student case study. Procedia CIRP 57:710–715. https://doi.org/10.1016/j.procir.2016.11.123

10. Ezeh OH, Susmel L (2018) On the fatigue strength of 3D-printed polylactide (PLA). Procedia Struct Integr 9:29–36. https://doi.org/10.1016/j.prostr.2018.06.007

11. Gordelier TJ, Thies PR, Turner L, Johanning L (2019) Optimising the FDM additive manufacturing process to achieve maximum tensile strength: a state-of-the-art review. Rapid Prototyp J 25(6):953–971. https://doi.org/10.1108/RPJ-07-2018-0183

12. Gomez-Gras G, Jerez-Mesa R, Travieso-Rodriguez JA, Lluma-Fuentes J (2018) Fatigue performance of fused filament fabrication PLA specimens. Mater Des 140:278–285. https://doi.org/10.1016/j.matdes.2017.11.072

13. Eyers DR, Potter AT, Gosling J, Naim MM (2018) The flexibility of industrial additive manufacturing systems. Int J Oper Prod Manag 38(12):2313–2343. https://doi.org/10.1108/IJOPM-04-2016-0200

14. Thomas D (2016) Costs, benefits, and adoption of additive manufacturing: a supply chain perspective. Int J Adv Manuf Technol 85:1857–1876. https://doi.org/10.1007/s00170-015-7973-6

15. Afrose MF, Masood SH, Iovenitti P, Nikzad M, Sbarski I (2016) Effects of part build orientations on fatigue behaviour of FDM-processed PLA material. Progress Addit Manuf 1(1–2):21–28. https://doi.org/10.1007/s40964-015-0002-3

16. Abeykoon C, Sri-Amphorn P, Fernando A (2020) Optimization of fused deposition modeling parameters for improved PLA and ABS 3D printed structures. Int J Lightweight Mater Manuf 3(3):284–297. https://doi.org/10.1016/j.ijlmm.2020.03.003

17. Morettini G, Razavi SMJ, Zucca G (2019) Effects of build orientation on fatigue behavior of Ti-6Al-4V as-built specimens produced by direct metal laser sintering. Procedia Struct Integr 24(2019):349–359. https://doi.org/10.1016/j.prostr.2020.02.032

18. Braccesi C, Morettini G, Cianetti F, Palmieri M (2018) Evaluation of fatigue damage with an energy criterion of simple implementation. Procedia Struct Integr 8:192–203. https://doi.org/10.1016/j.prostr.2017.12.021

19. Jaisingh SA, Harish K (2020) Fused Deposition modeling process parameters optimization and effect on mechanical properties and part quality: review and reflection on present research. Mater Today: Proc 21(3):1659–1672. https://doi.org/10.1016/j.matpr.2019.11.296

20. Dey A, Yodo N (2019) A systematic survey of FDM process parameter optimization and their influence on part characteristics. J Manuf Mater Process 3(3):64. https://doi.org/10.3390/jmmp3030064

21. Yao T, Deng Z, Zhang K, Li S (2019) A method to predict the ultimate tensile strength of 3D printing polylactic acid (PLA) materials with different printing orientations. Compos Part B: Eng 163(2):393–402. https://doi.org/10.1016/j.compositesb.2019.01.025

22. Corapi D, Morettini G, Pascoletti G, Zitelli C (2019) Characterization of a polylactic acid (PLA) produced by fused deposition modeling (FDM) technology. Procedia Struct Integr 24(2019):289–295. https://doi.org/10.1016/j.prostr.2020.02.026

23. Rajpurohit SR, Dave HK (2018) Effect of process parameters on tensile strength of FDM printed PLA part. Rapid Prototyp J 24(8):1317–1324. https://doi.org/10.1108/RPJ-06-2017-0134

24. Dev S, Srivastava R (2019) Experimental investigation and optimization of FDM process parameters for material and mechanical strength. Mater Today Proc 26:1995–1999. https://doi.org/10.1016/j.matpr.2020.02.435

25. Ezeh OH, Susmel L (2019) Fatigue strength of additively manufactured polylactide (PLA): effect of raster angle and non-zero mean stresses. Int J Fatigue 126(May):319–326. https://doi.org/10.1016/j.ijfatigue.2019.05.014

26. Tymrak BM, Kreiger M, Pearce JM (2014) Mechanical properties of components fabricated with open-source 3-D printers under realistic environmental conditions. Mater Des 58:242–246. https://doi.org/10.1016/j.matdes.2014.02.038

27. Cristian D (2017) Effect of raster orientation, infill rate pattern on the mechanical proprieties of 3D printed materials. ACTA Universitatis Cibiniensis. https://doi.org/10.1515/aucts-2017-0004

28. ASTM D638-14, Standard Test Method for Tensile Properties of Plastics, ASTM International, West Conshohocken, PA, 2014, www.astm.org

29. ASTM D7791-17, Standard Test Method for Uniaxial Fatigue Properties of Plastics, ASTM International, West Conshohocken, PA, 2017, www.astm.org

30. ASTM D5023-15, Standard Test Method for Plastics: Dynamic Mechanical Properties: In Flexure (Three-Point Bending), ASTM International, West Conshohocken, PA, 2015, www.astm.org

31. Lay M, Thajudin NLN, Hamid ZAA, Rusli A, Abdullah MK, Shuib RK (2019) Comparison of physical and mechanical properties of PLA, ABS and nylon 6 fabricated using fused deposition modeling and injection molding. Compos B Eng 176:107341. https://doi.org/10.1016/j.compositesb.2019.107341

32. ASTM D7774-17, Standard Test Method for Flexural Fatigue Properties of Plastics, ASTM International, West Conshohocken, PA, 2017, www.astm.org

33. Chartoff R, Joseph P, Menczel D, Dillman SH (2009) Dynamic mechanical analysis (DMA). Thermal analysis of polymers: fundamentals and applications. Wiley, pp 387–495

34. Menard KP, Menard N (2006) Dynamic mechanical analysis. Encyclopedia of Analytical chemistry: applications, theory and instrumentation, pp 1–25

35. BSI Standards Publication (2011) vulcanized or thermoplastic—determination of dynamic properties, Part 1: General guidance

36. Sharafi S, Li G (2016) Multiscale modeling of vibration damping response of shape memory polymer fibers. Compos B Eng 91:306–314. https://doi.org/10.1016/j.compositesb.2015.12.046ù

37. Rao S (2010) Mechanical Vibrations, 5th edn. University of Miami

38. Bledzki AK, Jaszkiewicz A, Scherzer D (2009) Mechanical properties of PLA composites with man-made cellulose and abaca fibres. Compos A 40:404–412

39. Wittbrodt B, Pearce JM (2015) The effects of PLA colour on material properties of 3-D printed components. Addit Manuf 8:110–116. https://doi.org/10.1016/j.addma.2015.09.006

40. Laureto JJ, Pearce JM (2018) Anisotropic mechanical property variance between ASTM D638–14 type I and type iv fused filament fabricated specimens. Polym Test 68(April):294–301. https://doi.org/10.1016/j.polymertesting.2018.04.029

41. Averett RD, Realff ML, Jacob K, Cakmak M, Yalcin B (2011) The mechanical behavior of poly (lactic acid) unreinforced and nanocomposite films subjected to monotonic and fatigue loading conditions. J Compos Mater 45(26):2717–2726. https://doi.org/10.1177/0021998311410464

42. Gebrehiwot SZ, Espinosa LL, Eickhoff JN, Rechenberg L (2021) The influence of stiffener geometry on flexural properties of 3D printed polylactic acid (PLA) beams. Progress Addit Manuf 6(1):71–81. https://doi.org/10.1007/s40964-020-00146-2

43. ASTM E739-10(2015) Standard Practice for Statistical Analysis of Linear or Linearized Stress-Life (S-N) and Strain-Life (ε-N) Fatigue Data, ASTM International, West Conshohocken, PA, 2015, www.astm.org

44. Safai L, Cuellar JS, Smit G, Zadpoor AA (2019) A review of the fatigue behavior of 3D printed polymers. Addit Manuf 28(March):87–97. https://doi.org/10.1016/j.addma.2019.03.023

45. Azadi M, Dadashi A, Dezianian S, Kianifar M, Torkaman S, Chiyani M (2021) High-cycle bending fatigue properties of additive-manufactured ABS and PLA polymers fabricated by fused deposition modeling 3D-printing. Forces Mech. https://doi.org/10.1016/j.finmec.2021.100016

46. Letcher T, Waytashek M (2014) Material property testing of 3D-printed specimen in PLA on an entry-level 3D printer. In: Proceedings of the ASME International Mechanical Engineering Congress and Exposition, Proceedings V02AT02A014

47. Sauer JA, Richardson GC (1980) Fatigue of polymers. Int J Fract Mech 16(6):499–532

48. Takemori MT (1984) Polymer fatigue. Annu Rev Mater Sci 14:171–204

Publisher's Note Springer Nature remains neutral with regard to jurisdictional claims in published maps and institutional affiliations.